Electrical Power and Energy Systems 110 (2019) 1–10

Contents lists available at ScienceDirect

Electrical Power and Energy Systems

journal homepage: www.elsevier.com/locate/ijepes

Reliability evaluation of power systems in the presence of energy storage system as demand management resource

Hejun Yang[a], Yeyu Zhang[a], Yinghao Ma[a,*], Ming Zhou[b], Xi Yang[a]

[a] School of Electrical Engineering and Automation, Hefei University of Technology, Hefei 230009, China
[b] The State Key Laboratory of Alternate Electrical Power System with Renewable Energy Sources (North China Electric Power University), Beijing 102206, China

ARTICLE INFO

Keywords:
Energy storage system
Demand management
Power system planning
PSO algorithm
Reliability evaluation

ABSTRACT

The energy storage system as a demand management resource can be incorporated into a power system for economizing the cost and improving the reliability. Therefore, this paper investigates the participation of energy storage system in demand management and its application to the reliability evaluation. Firstly, an optimal period partitioning model is proposed for dividing load series into the on-peak period, the mid-peak period, and the off-peak period, and a PSO based optimization algorithm is explored to optimize the unconstrained period partitioning problem which is transformed from the constrained optimization problem. Secondly, a demand management model with the participation of energy storage system is developed, and a peak shaving and valley filling factor is presented for describing the degree of demand management in this paper. Thirdly, a pseudo-analytical sampling method is presented for evaluating the reliability of the power system in the presence of energy storage system as a demand management resource, and some indices which can be used to describe the influence of demand management are defined. Finally, the Roy Billinton Test System and the Reliability Test System are conducted for verifying the correctness and validity of the proposed method.

1. Introduction

In recent years, the development and utilization of battery energy storage system (ESS) to satisfy the electrical demand has received considerable attention. Improvement in energy storage technologies will continue to encourage the use of energy storage system in power systems [1–5]. It is reported in [6–8] that the total energy capacity of ESS can range from about 2 MWh to 300 MWh. There are several advantages to incorporate an energy storage system into power system [9–12], such as (1) participating in demand management; (2) regulating the peak load and the system frequency; (3) storing the curtailed wind or solar energy; (4) smoothing real time power fluctuation of renewable energy generation, etc. Although the utilization of ESS in power system can provide a series of advantages, the utilization of ESS will directly affect the reliability of the power system. Therefore, this paper investigates the participation of ESS in demand management and its application to the reliability evaluation.

The energy storage system as a demand management resource, generally, can be regulated to discharge energy to the power system during the on-peak period and charge energy from power system during the off-peak period [13–15]. Thus, three periods (i.e., the on-peak period, the mid-peak period, and the off-peak period) should be divided firstly. These three periods are also considered in [16,17], but the period partitioning scheme is not thoroughly modeled but directly assumed. The *k*-means algorithm is often applied to power system [18], and also used in the period partitioning. But the partitioned results in [19] are always affected by random selection of all initial values.

In the existing literatures considering ESS [20–24], the ESS are generally used to attenuate the power fluctuation of renewable energy sources, such as wind energy, solar energy, and tidal energy. In [20], an optimization model of a solar-wind renewable energy system in the presence of ESS is presented. In [21,22], for the purpose of control and frequency regulation, ESS is utilized to smooth the wind power fluctuation. In [23], a control algorithm for joint demand response management and thermal comfort optimization in micro-grid composed of renewable energy sources and ESS is presented. Energy storage requirements for in-stream tidal generation on a limited capacity electricity grid are discussed in [24]. Except for reducing the power fluctuation of renewable energy as described above, ESS as a potential flexibility resource can be also used to directly participate in demand management to carry out load regulation strategy.

The reliability of power system with the integration of ESS has been

* Corresponding author.
E-mail addresses: cquyhj@126.com (H. Yang), zyy2017170250@163.com (Y. Zhang), yinghao_ma@126.com (Y. Ma), zhouming@ncepu.edu.cn (M. Zhou), yangxi@hfut.edu.cn (X. Yang).

https://doi.org/10.1016/j.ijepes.2019.02.042
Received 2 October 2018; Received in revised form 30 January 2019; Accepted 26 February 2019

Nomenclature

Constants

N_d	number of days in an entire year
c_1, c_2	acceleration coefficients
χ	contraction factor
$x_{\min}$, x_{max}	limits of position variables
$v_{\min}$, v_{max}	limits of velocity variables
Ψ	sampling duration
η_{sc}, η_{sd}	efficiency of energy storage system
E_{smax}	rated storage capacity
E_{smin}	minimum storage capacity
N_h	number of hours in one day
N_g	total number of sampling states
P_{sc}	rated charging power
P_{sd}	rated discharging power
T	hours for the entire year.
$P_{IC}(i)$	installed capacity of generator i
N_u	number of generators
R_{sg}	ratio of ESS's capacity to power plant's capacity

Variables

P_{on}, P_{mid}, P_{off}	decision variables of period partitioning problem
X_i	element of set $\{P_{on}, P_{mid}, P_{off}\}$
$x(k)$ ij	position variable for dimension j of particle i
$v(k)$ ij	velocity variable for dimension j of particle i
$P_{esc}(i, j)$	effective charging power at hour i of day j.
$P_{esd}(i, j)$	effective discharging power at hour i of day j
$E_s(i, j)$	real time stored energy at hour i of day j
$P_{src}(i, j)$	real time charging power
$P_{srd}(i, j)$	real time discharging power
$P_{am}(j)$	average load in mid-peak period of day j
$P_{Lmax}(j)$	maximum load of day j
$P_{Lmin}(j)$	minimum load of day j
r_{1ij}, r_{2ij}	random variables on [0, 1]
$b(k)$ ij	local position of particle i
$b(k)$ gj	global position among all particles
U_i	unavailability of generator i
A_j	availability of generator j

Sets

$\{o_l\}$	set of generators in the normal state
$\{f_l\}$	set of generators in the failure state

Functions

$I[\cdot]$	indicator function

Indices

$r_{ps}(j)$	peak shaving ratio index
$r_{vf}(j)$	valley filling ratio index
$r_{pv}(j)$	peak shaving and valley filling ratio index
$R_{I\text{-}before}$	reliability indices before considering DM
$R_{I\text{-}after}$	reliability indices after considering DM
LOLP	loss of load probability
LOLE	loss of load expectation
EENS	expected energy not supplied

investigated in [25–30]. In [25], ESS is utilized to supply power to isolated micro-grid for improving the system reliability, and a method for evaluating reliability of power distribution network is proposed. In [26], a model for calculating the optimal size of ESS in a micro-grid is presented, and the reliability index as a constraint function is considered into the optimal sizing problem of ESS. In [27], a stochastic framework for optimal sizing of ESS and reliability analysis of a hybrid power system is proposed, and ESS is designed to charge power from renewable energy sources and discharge power to the load for maintaining power balance. An effective probabilistic battery state model to enable implementation of reliability evaluation of renewable energy source based system integrated with battery storage is developed by [28]. A simulation technique is presented in [29] to evaluate the reliability of the power system with integrated wind energy and ESS, and some impacts on the reliability benefits from ESS are illustrated. In [30], the reliability assessment of generating systems containing wind power and ESS was analyzed, and the ESS was used to coordinate the wind energy for meeting the load demand.

As discussed above, ESS is incorporated into a power system for improving the system reliability through absorbing power from renewable sources and discharging power to load. However, it needs to further deeply investigate the impact of ESS as a flexible demand management resource on the reliability improvement of power system, especially to consider the peak shaving and valley filling factor into reliability modelling. In addition, due to the time series' characteristic of ESS, the sequential Monte Carlo technique was often used to evaluate the reliability of power system with the integration of ESS. However, because of the stochastic feature of sampling, results of reliability evaluation are fluctuant based on this method.

Based on the above analysis, firstly, aiming to overcome the uncertainty of the existing k-means clustering algorithm, a period partitioning optimization model is constructed in this paper, and a PSO algorithm with a constriction factor is utilized to search for the optimal solutions. Secondly, a demand side management scheme with the participation of ESS is established and a peak shaving and valley filling factor for describing the degree of participation of ESS in demand side management is designed. Thirdly, a reliability model including the peak shaving and valley filling factor is built and a pseudo-analytical sampling based reliability evaluation method is presented for considering the sequential charge – discharge process of ESS. In addition, several indices for describing the influence of demand management are defined in this paper. Finally, the Roy Billinton Test System (RBTS) and the Reliability Test System (RTS) are used to explore the correctness and validity of the proposed method.

The contributions of this paper are described as follows:

(1) An optimal period partitioning model is proposed for dividing load series into the on-peak, the mid-peak and the off-peak periods, and an unconstrained optimization problem is constructed to obtain optimal solutions.
(2) A demand side management scheme with the participation of energy storage system is built, and a peak shaving and valley filling factor for describing the degree of participation of energy storage system in demand side management is presented.
(3) A reliability model including the peak shaving and valley filling factor is established, and a pseudo-analytical sampling based reliability evaluation method considering sequential charge–-discharge process of ESS is presented. In addition, several indices for describing the influence of demand management are defined.

The remainder of the paper is organized as follows. Section 2 describes a PSO-based period partition optimization model. Section 3 presents the strategy of demand side management in the presence of energy storage system. Section 4 illustrates the reliability evaluation of

power systems in the presence of energy storage system as a demand side management resource. Case studies are presented in Section 5. The paper is summarized in Section 6.

2. A PSO based optimal period partitioning method

The energy storage system can be used as an effective demand management resource [31] to carry out a peak shaving and valley filling strategy, i.e., ESS can be used as a power source to supply energy to customer during the on-peak period and as consumer to absorb energy from the power system during the off-peak period. The period partitioning scheme has a direct impact on the demand management in the presence of ESS.

Thus, in this section, a period partitioning optimization model is first investigated. Then a penalty factor is incorporated into the proposed model for transforming the constrained optimization problem into an unconstrained optimization problem. Next, the PSO algorithm with a contraction factor is applied to the proposed model.

2.1. The objective function of optimization problem

Let $\{P_L(i, j),\ i = 1, 2, \ldots, N_h;\ j = 1, 2, \ldots, N_d\}$ be the hourly load sequence of day j, and $f(\cdot)$ be the objective function. An optimization model for partitioning the on-peak period, the mid-peak period, and the off-peak period can be given by

$$\min\left\{f(P_{on}, P_{mid}, P_{off}) = \sqrt{\frac{1}{N_h}\sum_{i=1}^{N_h}(P_L(i,j) - X(i))^2}\right\}, \tag{1}$$

$$s.t.\ \begin{cases} X(i) \in \{P_{on}, P_{mid}, P_{off}\} \\ P_{L\min}(j) \leqslant P_{on}, P_{mid}, P_{off} \leqslant P_{L\max}(j) \end{cases}. \tag{2}$$

2.2. The fitness function of optimization problem

The constrained optimization problem can be transformed to an unconstrained optimization problem through incorporating a penalty function in the objective function. Let $J(P_{on}, P_{mid}, P_{off})$ denote a penalty function. A fitness function including a penalty function is given by

$$F(P_{on}, P_{mid}, P_{off}) = f(P_{on}, P_{mid}, P_{off}) + J(P_{on}, P_{mid}, P_{off}). \tag{3}$$

The penalty function $J(\cdot)$ [32] can be expressed as

$$J(\cdot) = \varphi(k) \times \sum_{i=1}^{m}(\theta(q_i(\cdot)) \times q_i(\cdot)^{\gamma(q_i(\cdot))}), \tag{4}$$

$$q_i(\cdot) = \max\{0, -h_i(\cdot)\}, \tag{5}$$

where k denotes the algorithm's current iteration number. $\varphi(k)$ is a dynamically modified penalty value. m is the number of constraint functions. $h_i(\cdot)$ is the i^{th} constraint function expressed by

$$\begin{cases} h_1(P_{on}) = (P_{L\max}(j) - P_{on})(P_{on} - P_{L\min}(j)) \geqslant 0 \\ h_2(P_{mid}) = (P_{L\max}(j) - P_{mid})(P_{mid} - P_{L\min}(j)) \geqslant 0 \\ h_3(P_{off}) = (P_{L\max}(j) - P_{off})(P_{off} - P_{L\min}(j)) \geqslant 0 \end{cases}. \tag{6}$$

The functions $\theta(\cdot)$ and $\gamma(\cdot)$ [32] is given by

$$\gamma(q_i(\cdot)) = \begin{cases} 1 & q_i(\cdot) < 1 \\ 2 & q_i(\cdot) \geqslant 1 \end{cases}, \tag{7}$$

$$\theta[q_i(\cdot)] = \begin{cases} 10 & q_i(\cdot) < 0.01 \\ 20 & 0.01 \leqslant q_i(\cdot) < 0.1 \\ 100 & 0.1 \leqslant q_i(\cdot) < 1 \\ 300 & other \end{cases}. \tag{8}$$

2.3. Optimization method

Since the PSO algorithm can search for the optimal solution in a continuous real solution space [33,34]. Thus, it is adopted here to solve the optimization problem described above.

In the fitness function, P_{on}, P_{mid}, and P_{off} are decision variables, while the decision variables in the PSO based optimization problem are re-expressed by position variables $x(k)\ ij (j = 1, 2, 3)$. The solving process of the optimization problem can be described as follows.

Step 1: Initialize the position variable $x(k)\ ij (j = 1, 2, 3)$ and the velocity variable $v(k)\ ij$ by Eq. (9), and calculate the local optimal position $b(k)\ ij$ and the global optimal position $b(k)\ gj$ for all particles.

$$\begin{cases} x_{ij}^{(k)} = r_{1ij}(x_{\max} - x_{\min}) + x_{\min} \\ v_{ij}^{(k)} = r_{2ij}(v_{\max} - v_{\min}) + v_{\min} \end{cases}, \tag{9}$$

Step 2: Update the position variable $x(k+1)\ ij$ and the velocity variable $v(k+1)\ ij$ for all particles by

$$\begin{cases} v_{ij}^{(k+1)} = \chi\{v_{ij}^{(k)} + c_1 r_{1ij}^{(k)}[b_{ij}^{(k)} - x_{ij}^{(k)}] + c_2 r_{2ij}^{(k)}[b_{gj}^{(k)} - x_{ij}^{(k)}]\} \\ x_{ij}^{(k+1)} = x_{ij}^{(k)} + v_{ij}^{(k+1)} \end{cases}, \tag{10}$$

Step 3: According to the Eq. (3), calculate the fitness value $F(x(k+1)\ ij)$ corresponding to each position variable $x(k+1)\ ij$ in the $(k+1)^{\text{th}}$ iteration.

Step 4: Update the local optimal position $b(k+1)\ ij$ and the global optimal position $b(k+1)\ gj$. Compare the fitness value $F(x(k+1)\ ij)$ with the local optimal fitness value $F(b(k)\ ij)$. If $F(x(k+1)\ ij) < F(b(k)\ ij)$, then $b(k+1)\ ij = x(k+1)\ ij$; otherwise $b(k+1)\ ij = b(k)\ ij$. Compare the local optimal fitness value $F(b(k+1)\ ij)$ with the global optimal fitness value $F(b(k)\ gj)$. If $F(b(k+1)\ ij) < F(b(k)\ gj)$, then $b(k+1)\ gj = b(k+1)\ ij$; otherwise, $b(k+1)\ gj = b(k)\ gj$.

Step 5: Terminate the iteration if the convergence criterion is satisfied, and output the global optimal position; otherwise, $k = k + 1$, and go to S2.

The flow chart for describing the period partitioning of the on-peak, mid-peak, and off-peak periods is illustrated in Fig. 1.

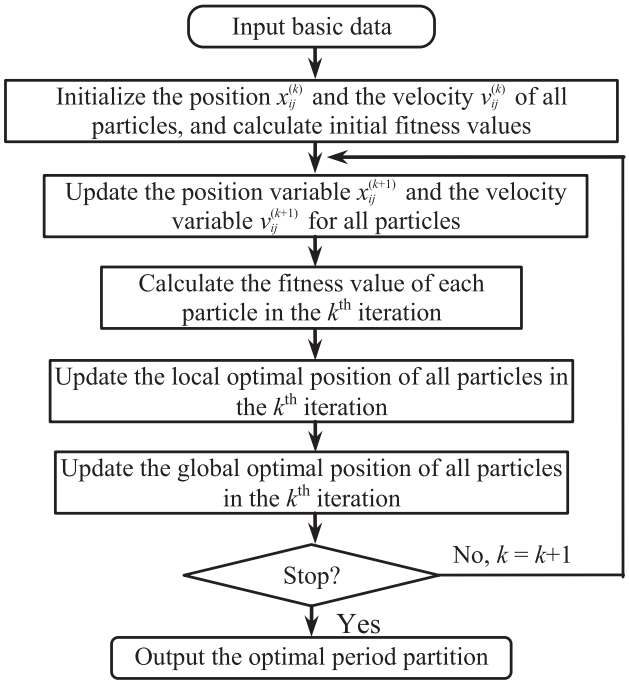

Fig. 1. Flowchart of period partitioning for the on-peak, mid-peak, and off-peak periods.

3. ESS modelling as a demand management resource

The energy storage system as a demand management resource can effectively smooth the load curve by regulating its operation modes, i.e., ESS can be controlled to operate in a discharging mode during the on-peak period and a charging mode during the off-peak period. However, the real time charging-discharging power is limited by the rated storage capacity, the rated charging power, and the rated discharging power. Thus, operation modes of energy storage system are investigated and a factor for reflecting the degree of demand management is presented in this section.

3.1. Energy storage system model

An effective charging power variable $P_{esc}(i, j)$ and an effective discharging power variable $P_{esd}(i, j)$ at the i^{th} hour can be defined by

$$P_{esc}(i,j)=\begin{cases}\frac{(E_s(i-1,j)-E_{s\min})}{\psi}, & \frac{(E_s(i-1,j)-E_{s\min})}{\psi}\leqslant P_{sd}\\ P_{sd}, & \frac{(E_s(i-1,j)-E_{s\min})}{\psi}> P_{sd}\end{cases}, \tag{11}$$

$$P_{esd}(i,j)=\begin{cases}\frac{(E_{s\max}-E_s(i-1,j))}{\psi}, & \frac{(E_{s\max}-E_s(i-1,j))}{\psi}\leqslant P_{sc}\\ P_{sc}, & \frac{(E_{s\max}-E_s(i-1,j))}{\psi}> P_{sc}\end{cases}. \tag{12}$$

When the lower and upper limits of the storage capacity are considered, the real time stored energy variable $E_s(i, j)$ [35] can be obtained by

$$E_s(i,j)=\begin{cases}E_{s\min}, & E_{sv}(i,j)<E_{s\min}\\ E_{sv}(i,j), & E_{s\min}\leqslant E_{sv}(i,j)\leqslant E_{s\max},\\ E_{s\max}, & E_{sv}(i,j)>E_{s\max}\end{cases} \tag{13}$$

where $E_{sv}(i, j)$ is calculated by

$$E_{sv}(i,j)=\begin{cases}E_s(i-1,j)+\psi\eta_{sc}P_{rsc}(i,j), i\in charging\\ E_s(i-1,j)-\psi\frac{P_{rsd}(i,j)}{\eta_{sd}}, i\in discharging\end{cases}. \tag{14}$$

3.2. Degree of participation of ESS in demand side management

The time series load curve of one day is drawn in Fig. 2. In Fig. 2, $P_L(i,j)$ and $P_{La}(i,j)$ are the load power of hour i of day j before and after carrying out the demand management. For avoiding excessive charging and discharging, a peak shaving and valley filling factor S_v is defined by

$$S_v=\frac{\Delta P(i,j)}{P_L(i,j)-P_{am}(j)}. \tag{15}$$

where $\Delta P(i,j)$ is the load power difference between before and after considering the demand management. Generally, S_v is given in advance. Then, $\Delta P(i,j)$ can be calculated by

$$\Delta P(i,j)=S_v\times[P_L(i,j)-P_{am}(j)]. \tag{16}$$

where $P_{am}(j)$ is the average load of the mid-peak period for day j. It is given by

$$P_{am}(j)=\frac{1}{m_{mid}}\sum_{i=1}^{m_{mid}}P_L(i,j),\ i\in mid\ -\ peak. \tag{17}$$

After considering the influence of the effective charging-discharging power and the peak shaving and valley filling factor, the real time charging power and discharging power can be simulated by

$$P_{srd}(i,j)=\begin{cases}\Delta P(i,j) & 0\leqslant\Delta P(i,j)<P_{sed}(i,j)\\ P_{sed}(i,j) & \Delta P(i,j)\geqslant P_{sed}(i,j)\end{cases} \tag{18}$$

$$P_{src}(i,j)=\begin{cases}-\Delta P(i,j) & 0\leqslant-\Delta P(i,j)<P_{\boldsymbol{sec}}(i,j)\\ P_{\boldsymbol{sec}}(i,j) & \Delta P(i,j)\geqslant P_{\boldsymbol{sec}}(i,j)\end{cases} \tag{19}$$

The real series load power after considering ESS's participation in demand management is given by

$$P_{La}(i,j)=\begin{cases}P_L(i,j)-P_{srd}(i,j) & i\in on\ -\ peak\\ P_L(i,j) & i\in mid\ -\ peak\\ P_L(i,j)+P_{src}(i,j) & i\in off\ -\ peak\end{cases} \tag{20}$$

4. Reliability evaluation of power system in the presence of energy storage system as demand management

The energy storage system can not only smooth the load curve but also affect the reliability of the power system. Thus, a pseudo-analytical technique is proposed for incorporating demand management in the presence of ESS into the reliability evaluation of power system, and several indices are defined in this section.

The pseudo-analytical technique is introduced as follows: Firstly, the power system states are sampled based on an analytical technique. Secondly, the sequential charging-discharging process of ESS is simulated under each state of the power system. Finally, reliability indices are evaluated.

4.1. Reliability evaluation indices

The power system reliability considering the participation of ESS in demand management is investigated in this paper. The annual reliability indices of power system under the consideration are the loss of load probability $LOLP(S_v)$, the loss of load expectation $LOLE(S_v)$, and the expected energy not supplied $EENS(S_v)$. They can be calculated by

$$LOLP(S_v)=\frac{1}{N_dN_h}\sum_{l=1}^{N_g}\left\{\left(\prod_{i\in\{o_l\}}U_i\prod_{j\in\{f_l\}}A_j\right)\times\sum_{j=1}^{N_d}\sum_{i=1}^{N_h}I[P_L(i,j)(1-S_v)+P_{am}(j)S_v>P_G(l)]\right\} \tag{21}$$

$$LOLE(S_v)=\frac{T}{N_dN_h}\sum_{l=1}^{N_g}\left\{\left(\prod_{i\in\{o_l\}}U_i\prod_{j\in\{f_l\}}A_j\right)\times\sum_{j=1}^{N_d}\sum_{i=1}^{N_h}I[P_L(i,j)(1-S_v)+P_{avm}(j)S_v>P_G(l)]\right\} \tag{22}$$

$$EENS(S_v\%)=\sum_{l=1}^{N_g}\left\{\left(\prod_{i\in\{o_l\}}U_i\prod_{j\in\{f_l\}}A_j\right)\sum_{j=1}^{N_d}\sum_{i=1}^{N_h}\frac{T[P_L(i,j)-P_G(l)]}{N_dN_h}\times I[P_L(i,j)(1-S_v)+P_{avm}(j)S_v>P_G(l)]\right\} \tag{23}$$

where $I[\cdot]$ is the indicator function, $I[\cdot]=1$ if $P_L(i,j)(1-S_v)+P_{avm}(j)\times S_v>P_G(l)$; otherwise, $I[\cdot]=0$.

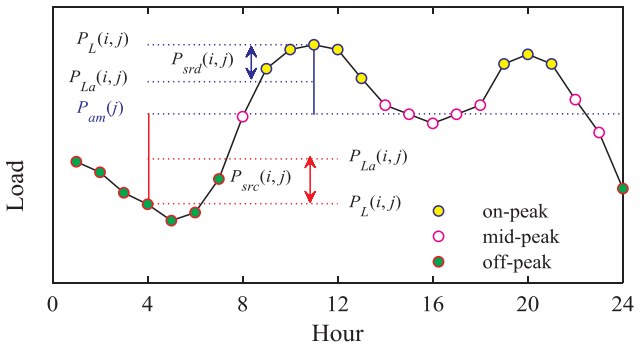

Fig. 2. Time series load curve of one day.

The improvement degree of reliability indices (I_{rd}) can be given by

$$I_{rd} = \frac{R_{I-before} - R_{I-after}}{R_{I-after}} \times 100, \tag{24}$$

where $R_{I\text{-}before}$ and $R_{I\text{-}after}$ are the reliability indices before and after considering demand management. R_I denotes the any reliability index, i.e., $LOLP(S_v)$, $LOLE(S_v)$, or $EENS(S_v)$.

4.2. Indices of demand management considering participation of ESS

In this paper, several indices for describing the influence of ESS's participation in demand management are defined, i.e., the peak shaving ratio index $r_{ps}(j)$, the valley filling ratio index $r_{vf}(j)$, and the peak shaving and valley filling ratio index $r_{pv}(j)$.

$$r_{ps}(j) = \frac{P_{L\max}(j) - P_{am}(j)}{P_{am}(j)}, \tag{25}$$

$$r_{vf}(j) = \frac{P_{am}(j) - P_{L\min}(j)}{P_{am}(j)}, \tag{26}$$

$$r_{pv}(j) = \frac{P_{L\max}(j) - P_{L\min}(j)}{P_{am}(j)}. \tag{27}$$

The ratio of the rated storage capacity of ESS to the installed capacity of power plant (R_{sg}) is defined by

$$R_{sg} = \frac{E_{s\max}}{\sum_{i=1}^{N_u} P_{IC}(i)} \times 100. \tag{28}$$

4.3. Reliability evaluation technique

A pseudo-analytical technique is utilized to evaluate the reliability of power system considering the demand management in the presence of ESS. The reliability evaluation process is described as follows, and the corresponding flowchart is described in Fig. 3.

Step1: Input basis data including the load series, the parameters of energy storage device, the RBTS and the RTS data, etc.

Step2: Obtain the optimal period partition of each day, i.e., partitioning for the on-peak period, the mid-peak period, and the off-peak period for each day. Let $l = 1$.

Step3: Enumerate the l^{th} generation state of power system on the basis of the failure rate and the repair time of each generator. Let $i = 1$.

Step4: According to daily load curves of the whole year, partitioned periods of each day, demand management strategies, and ESS's operation modes, simulate the sequential charging-discharging process of ESS and calculate the i^{th} hourly load power after considering demand management.

Step5: Compare the l^{th} generation capacity with the i^{th} hourly load power, and calculate the reliability under the condition of this operation state.

Step6: Continue to compare the next operation state until all load power is traversed.

Step7: Terminate the simulation process if all generation states are enumerated; otherwise, let $l = l + 1$ and go to Step3.

5. Case studies

In this paper, the RTS and the RBTS are used to investigate the reliability of power system considering the participation of ESS in demand management. The RBTS includes 11 generators having a total installed capacity of 240 MW, and the RTS includes 32 generators having a total installed capacity of 3405 MW. The time series load data which has a peak load of 185 MW for the RBTS and 2850 MW for the RTS is used. The reliability parameter of the two test systems can be found in [36]. The parameters of energy storage system is set by: the rated storage capacity $E_{smax} = 50$ MWh, the rated charging power $P_{sc} = 25$ MW, and the rated discharging power $P_{sd} = 25$ MW, and the peak shaving and valley filling factor $S_v = 0.3$.

The proposed method was implemented in the Microsoft Visual Studio 2013 C++ environment on a PC with 2.50 GHz Intel(R) Core (TM) i7 CPU, 8 GB RAM and 64 bit operating system.

5.1. Period partitioning

The daily load curve of an entire year is applied to the proposed period partitioning method. The optimal period partitioning for all days (total 364 days for an entire year) have been obtained and daily load curves for all days can be also drawn. Due to the space limit, only take the load curves of four different seasons as examples to display the results of the period partitioning. In this section, the load curves of March (65th day), June (155th day), September (245th day), and December (335th day) are depicted in Fig. 4.

It can be observed from Fig. 4 that the load in the on-peak period is always larger than the load in the mid-peak period, and the load in the off-peak period is always smaller than the load in the mid-peak period. For Fig. 4(a), the on-peak period includes hours of 9–13 and 19–21, and the hours of mid-peak period is from 14 to 18, 22–23, and 8, the off-peak period from 1 to 7 and 24. Similar patterns of the period partitioning can be found from other months, so not all the months are drawn.

In this paper, one hundred particles are designed to search for optimal solutions. The iteration processes of the proposed period partitioning method for independent running of ten times are depicted in Fig. 5, and the corresponding optimal fitness values are listed in Table 1. It can be observed from Fig. 5 that the iteration processes approximately tends to be stable after the iteration number of about 60 for these four months. Therefore, the proposed period partitioning method is efficient to optimize the periods.

Fig. 6 depicts the time-consuming of optimization process for independent running of ten times. Fig. 7 shows the average time-consuming for the months of March, June, September and December. It can be observed from Figs. 6 and 7 that the average time-consuming for the months of March, June, September and December are 18.4 ms, 19.1 ms, 18.9 ms, and 19.3 ms, respectively. And the average time-consuming for the four months is 18.925 ms. Thus, the optimization efficiency is adequate.

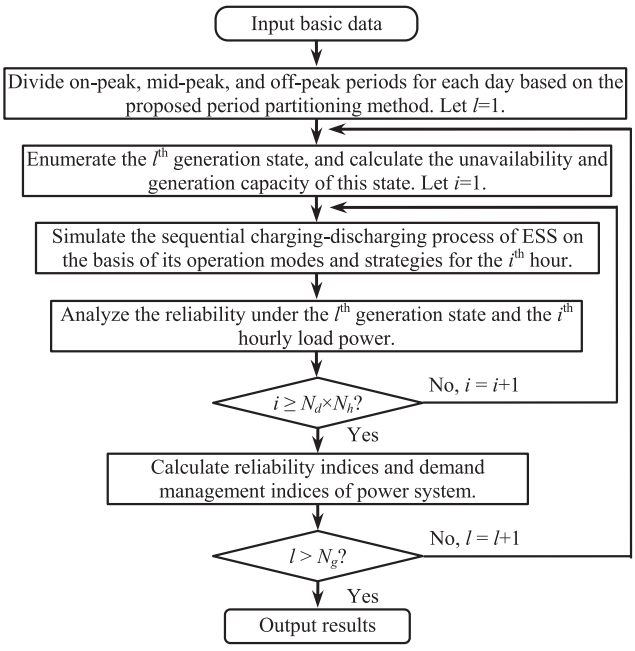

Fig. 3. Flowchart of the reliability evaluation process.

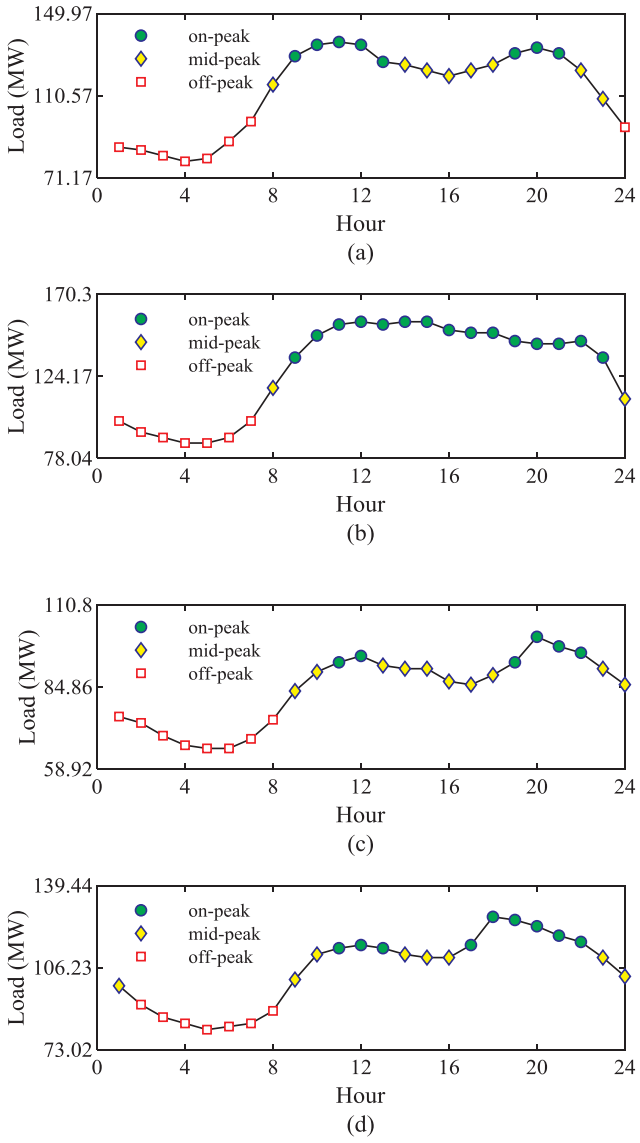

Fig. 4. Period partitioning for (a) March, (b) June, (c) September, and (d) December.

Experiments for the problem are independently conducted for 1000 times based on the PSO method and the *k*-means algorithm, respectively. Table 2 shows experimental results. It can be seen that fitness values obtained by *k*-means are fluctuant while that of the PSO method is constant and the minimum fitness value of *k*-means is completely same as fitness value of the PSO method. Thus, the PSO method is efficient for the period partitioning problem.

5.2. Load curve after considering the participation of ESS in demand management

The four days, i.e., March (65th day), June (155th day), September (245th day), and December (335th day), are also as example to analyze the influence of the ESS's participation in demand management. The load variations before and after considering ESS are described in Fig. 8 for comparisons. Fig. 8(a) displays the load variation for March, and Fig. 8(b) shows the real time stored energy of ESS corresponding to Fig. 8(a). Similarly, Fig. 8(c) and (d) describe the load variation and the real time stored energy for June, Fig. 8(e) and (f) for September, Fig. 8(g) and (h) for December. In legend of Fig. 8, "on-peak Bf", "mid-peak Bf", and "off-peak Bf" denote the periods before considering the

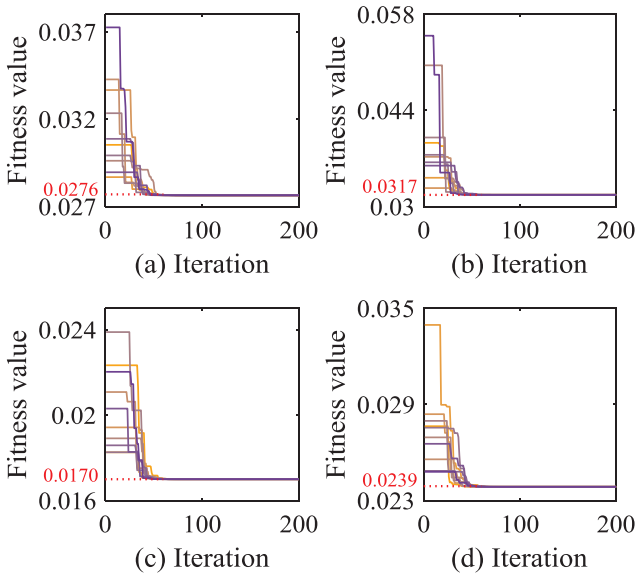

Fig. 5. The iteration processes: (a) for March, (b) for June, (c) for September, and (d) December.

Table 1
Optimal fitness values and the decision variables of different months.

Month	Fitness Value	P_{on}	P_{mid}	P_{off}
Mar.	0.0276	0.7149	0.6513	0.4689
Jun.	0.0317	0.7957	0.6194	0.4974
Sep.	0.0170	0.5173	0.4775	0.3777
Dec.	0.0239	0.6427	0.5791	0.4611

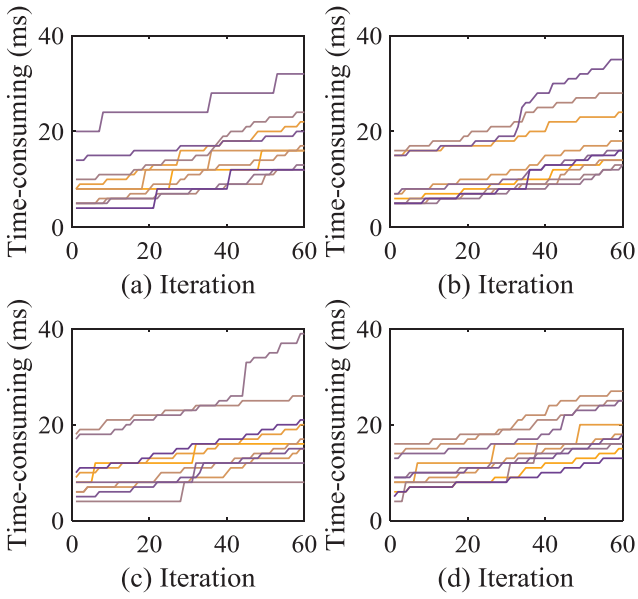

Fig. 6. The time-consuming of optimization process of: (a) March, (b) June, (c) September, and (d) December.

demand management, and "on-peak Af", "mid-peak Af", and "off-peak Af" denote the periods after considering the demand management.

It can be observed from Fig. 8(a) and (b) that: (1) For the on-peak period, the load curve after considering the demand management is located below the load curve before considering the demand management. The reason for the reduction of load power is that the ESS is in the discharging state during the on-peak period, i.e., the ESS as power source supplies energy to load. And the real time stored energy shown

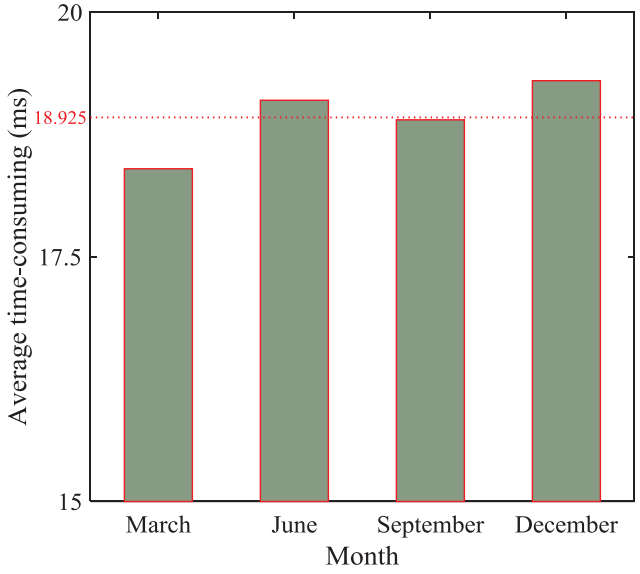

Fig. 7. The average time-consuming for (a) March, (b) June, (c) September, and (d) December.

Table 2
Comparison of fitness values for the PSO and the *k*-means.

Month	PSO	*k*-means		
		Minimum	Average	Maximum
Mar.	0.0276	0.0276	0.0286	0.0298
Jun.	0.0317	0.0317	0.0339	0.0375
Sep.	0.0170	0.0170	0.0181	0.0209
Dec.	0.0239	0.0239	0.0246	0.0253

in Fig. 8(b) is gradually declining in this period. (2) For the mid-peak period, according to the operation strategy, the ESS is in the idle state (i.e., it is in a no-charging and no-discharging state). Thus, the two load curves are always overlapped and the real time stored energy is always parallel to the horizontal axis for the mid-peak period. (3) For the off-peak period, Fig. 8(b) shows that the real time stored energy increases for the 1th, 2th, and 24th hours. Thus Fig. 8(a) displays that the load curve after considering demand management is located above the load curve before considering demand management. However, for the other hours of the off-peak period, the two load curves are observed to be overlapped due to the limit of the rated storage capacity.

Fig. 8(c)–(h) show the similar features. In the on-peak period, as the ESS is in the discharging state, the load power will be able to descend. In the mid-peak period, as the ESS is in the idle state, the load power keeps invariable. But, in the off-peak period, the ESS is in the charging state, thus the load curves will be able to ascend. During the entire charging and discharging process, the demand management is limited by the maximum storage capacity, the maximum charging power, and the maximum discharging power.

According to the above discussion, the ESS as a demand management resource can effectively decrease the load demand during on-peak period and increases the customer's energy consumer during off-peak period.

5.3. Reliability evaluation considering the participation of ESS in demand management

The ESS is integrated into the RBTS and the RTS for investigating the influence of demand management. The reliability indices of the RBTS and the RTS before and after considering the participation of ESS in demand management are listed in Table 3. It can be seen from

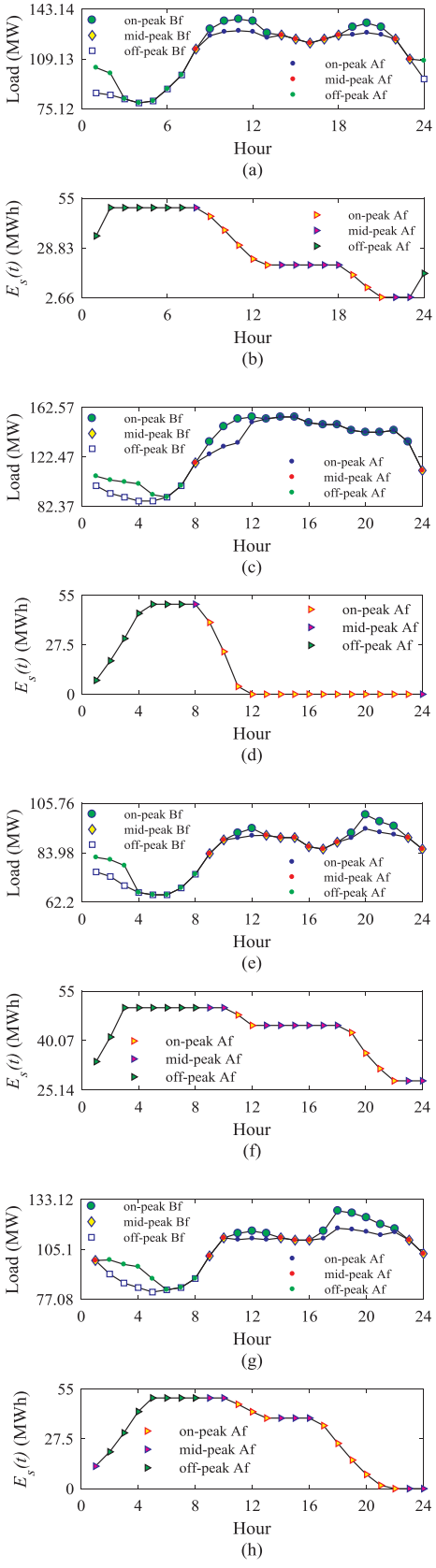

Fig. 8. Load variation and state of charge before and after considering ESS: (a) and (b) for March, (c) and (d) for June, (e) and (f) for September, (g) and (h) for December.

Table 3
Reliability indices of power systems with and without considering ESS.

Indices	RBTS			RTS		
	LOLP	*LOLE*	*EENS*	*LOLP*	*LOLE*	*EENS*
Be-ESS	1.25E−04	1.09	9.85	1.07E−03	9.41	1177.60
Af-ESS	9.36E−05	0.82	7.40	1.05E−03	9.22	1146.19
I_{rd} (%)	24.88	24.88	24.91	2.03	2.03	2.67
R_{sg} (%)	20.83			1.47		

"Be-ESS" denotes "before considering ESS; "Af-ESS" denotes "after considering ESS".

Table 4
The demand management indices in the presence of ESS.

Date	Before ESS			After ESS		
	r_{ps}(%)	r_{vf}(%)	r_{pv}(%)	r_{ps}(%)	r_{vf}(%)	r_{pv} (%)
Mar.	13.154	34.371	47.525	6.577	34.371	40.948
Jun.	35.135	24.324	59.460	35.135	21.621	56.757
Sep.	14.026	25.884	39.909	7.013	25.884	32.896
Dec.	18.344	24.260	42.604	9.172	23.077	32.249

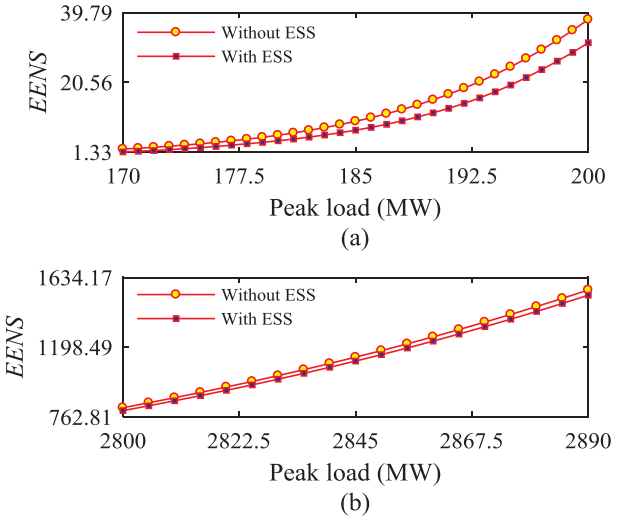

Fig. 9. The influence of the peak load on the reliability of the power system with and without ESS.

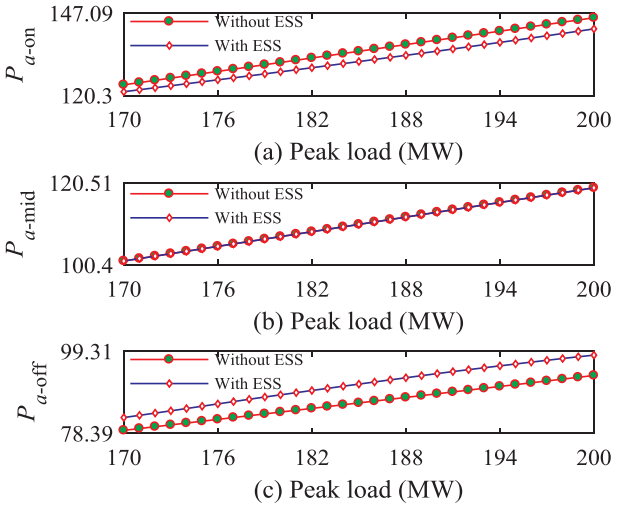

Fig. 10. Average load of (a) on-peak period, (b) mid-peak period, and (c) off-peak period under different peak load.

Table 3 that the *LOLP* index for the RBTS is improved from 0.000125 to 0.0000936 with the descent of 24.88% and for the RTS is from 0.00107 to 0.00105 with the descent of 2.03%. For the *EENS* index, the RBTS has an improvement of 24.91% from 9.85 MWh to 7.40 MWh and the RTS is 2.67% from 1177.60 MWh to 1146.19 MWh. As the ratios of the rated storage capacity to the installed capacity of test systems are 20.83% for the RBTS and 1.47% for the RTS, respectively, the percentage of reliability improvement of the RBTS is obviously higher than that of the RTS.

Therefore, the participation of ESS in demand management can not only reduce the difference between the peak load and the valley load but also obviously improve the reliability of the power system.

The demand management indices before and after considering energy storage system are listed in Table 4. It can be seen from Table 4 that: (1) for r_{ps} index, as the ESS can supply a part of energy to the load during the off-peak period, thus r_{ps} has an obvious decrease for the four months; (2) for r_{vf} index, due to the limitation of maximum energy capacity, this index is invariable before and after considering ESS for the months of March and September. But it reduces in the months of June and December; (3) the r_{pv} index for the four months decreases due to the reduction of difference between the maximum load and the minimum load. Therefore, the demand management in the presence of ESS can decrease the on-peak period load and increase the off-peak period load.

The influences of the peak load on the reliability of the power system with and without considering ESS are shown in Fig. 9(a) for the RBTS and Fig. 9(b) for the RTS. It can be observed from Fig. 9 that the *EENS* index for both the RBTS and the RTS is gradually increasing with the increasing peak load. The *EENS* index curve of considering ESS is always below that of without considering ESS, and the difference between the two curves is more and more obvious. This also verifies that the participation of ESS in demand management can effectively improve the reliability of the power system.

The average load curves of the on-peak period, the mid-peak period, and the off-peak period under different peak load values are depicted in Fig. 10. The variables $P_{a\text{-}on}$, $P_{a\text{-}mid}$, and $P_{a\text{-}off}$ are the average load power of the on-peak period, the mid-peak period, and the off-peak period, respectively. Fig. 10(a) shows that the average load of the on-peak period becomes smaller when the demand management is considered, while it is just opposite to that of the off-peak period which is shown in Fig. 10(c). As the ESS keeps invariable during the mid-peak period, the two curves shown in Fig. 10(b) are overlapped.

5.4. The influence of factors on the reliability of the power system

5.4.1. The influence of the peak shaving and valley filling factor

The peak shaving and valley filling factor S_v can be changed for adjusting operation strategies. In order to investigate its influence on the reliability, the value of S_v changes from 0 to 2 with an increase of 0.01. The *EENS* index is taken as an example. The results are shown in Fig. 11(a) for the RBTS and Fig. 11(b) for the RTS. It can be observed from Fig. 11 that with the increasing value of S_v, the *EENS* index first descends rapidly and then rises slightly until it remains stable. The values of S_v corresponding to the smallest *EENS* values for the RBTS and the RTS are 0.3 and 0.02, respectively.

Therefore, the peak shaving and valley filling factor has a significant influence on the reliability of the power system. In a practical power system, a reasonable selection of the peak shaving and valley filling factor can make the power system more reliable.

5.4.2. Influence of parameters of ESS

The *EENS* index is also taken as an example to investigate the influences of the rated storage capacity, the rated charging power, and the rated discharging power on the reliability. The results are shown in Fig. 12. It can be seen from Fig. 12(a) and (b) that *EENS* index is first gradually decreasing and then trend to be stable when E_s and P_{sc} are

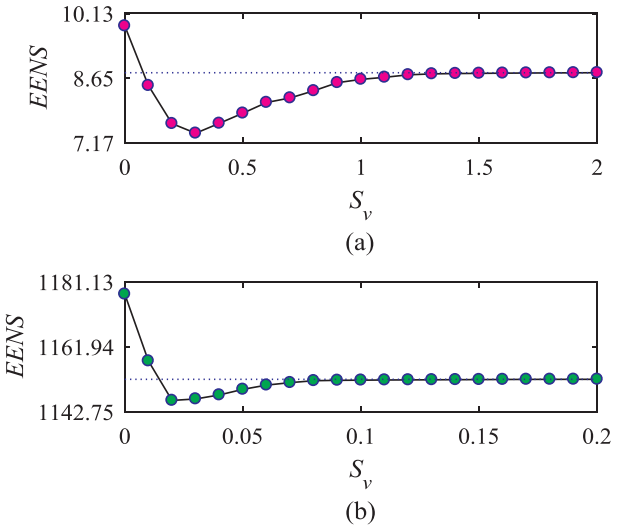

Fig. 11. Influence of S_v on the reliability of power system: (a) for the RBTS; (b) for the RTS.

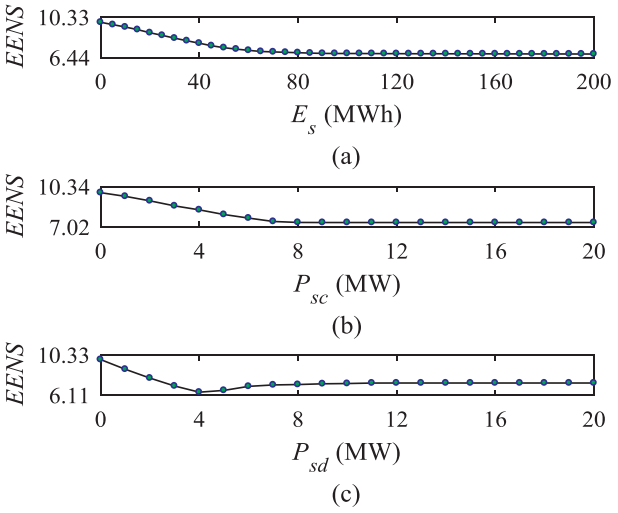

Fig. 12. Influence of parameters on reliability: (a) for rated storage capacity, (b) for rated charging power, and (c) for rated discharging power.

approximate to 80 MWh and 8 MW. For Fig. 12(c), the *EENS* index descends firstly and then rises slightly until it remains invariable. Therefore, different ESS parameters have different reliability levels, and for a given power system, an optimal selection of the parameters can be carried out to improve the reliability of the power system.

6. Conclusion

This paper proposes a period partitioning optimization model and constructs an unconstrained optimization problem on the basis of the constrained optimization problem. A demand management model with the participation of an energy storage system is investigated in this paper. A peak shaving and valley filling factor and several indices are presented for describing the degree of demand management of participation of an energy storage system. A pseudo-analytical sampling based reliability evaluation method is presented for considering the sequential charge – discharge process of ESS. The proposed method has been applied to the RBTS and the RTS. The results of case studies can be summarized as follows:

(1) The proposed period partitioning model is effective and efficient for the division of on-peak period, the mid-peak period, and the off-peak period.
(2) The energy storage system as a demand management resource can be effectively carried out for decreasing the difference between the peak load and valley load and improving the reliability of the power system.
(3) The peak shaving and valley filling factor presented in this paper has a significant influence on the reliability of the power system. An optimal peak shaving and valley filling factor which can make the power system more reliable can be designed for the practical electric power system.
(4) The parameters of energy storage system have a direct influence on the reliability of power system, and carrying out the selection of the parameters can improve the reliability of the power system.

The proposed technique can conveniently incorporate the energy storage system as a demand management resource into the reliability evaluation of a power system. In addition, an optimal peak shaving and valley filling factor for improving the reliability of power system can be also obtained based on the proposed method.

Acknowledgement

This work was supported in part by the National Natural Science Foundation of China under Grant 51607051, Anhui Provincial Natural Science Foundation under Grant 1708085ME107, and the State Key Laboratory of Alternate Electrical Power System with Renewable Energy Sources under Grant LAPS18011.

References

[1] Abdulla K, Hoog J, Muenzel V, et al. Optimal operation of energy storage systems considering forecasts and battery degradation. IEEE Trans Smart Grid 2018;9(3):2086–96.
[2] Betzin C, Wolfschmidt H, Luther M. Electrical operation behavior and energy efficiency of battery systems in a virtual storage power plant for primary control reserve. Int J Electr Power Energy Syst 2018;97:138–45.
[3] Kazemi M, Zareipour H. Long-term scheduling of battery storage systems in energy and regulation markets considering battery's lifespan. IEEE Trans Smart Grid 2018;9(6):6840–9.
[4] Korkas CD, Baldi S, Kosmatopoulos EB. Grid-connected microgrids: demand management via distributed control and human-in-the-loop optimization. Adv Renew Energy Power Technol 2018;2:315–44.
[5] Cortés A, Mazón J, Merino J. Strategy of management of storage systems integrated with photovoltaic systems for mitigating the impact on LV distribution network. Int J Electr Power Energy Syst 2018;103:470–82.
[6] Zhu Y, Liu C, Sun K, Shi D, Wang Z. Optimization of battery energy storage to improve power system oscillation damping. IEEE Trans Sustain Energy 2018. [Early Access].
[7] Zhang C, Wei Y, Cao P, et al. Energy storage system: current studies on batteries and power condition system. Renew Sust Energ Rev 2018;82:3091–106.
[8] Suberu MY, Mustafa MW, Bashir N. Energy storage systems for renewable energy power sector integration and mitigation of intermittency. Renew Sust Energ Rev 2014;35:499–514.
[9] Ren G, Ma G, Cong N. Review of electrical energy storage system for vehicular applications. Renew Sust Energ Rev 2015;41:225–36.
[10] Ghasemi A, Enayatzare M. Optimal energy management of a renewable-based isolated microgrid with pumped-storage unit and demand response. Renew Energy 2018;123:460–74.
[11] Zhao H, Wu Q, Hu S, Xu H, Rasmussen CN. Review of energy storage system for wind power integration support. Appl. Energy 2015;137:545–53.
[12] Faisal M, Hannan MA, Ker PJ, Hussain A, Mansor M, Blaabjerg F. Review of energy storage system technologies in microgrid applications: issues and challenges. IEEE Access 2018;6:35143–64.
[13] Aalami HA, Nojavan S. Energy storage system and demand response program effects on stochastic energy procurement of large consumers considering renewable generation. IET Gener Transm Distrib 2016;10(1):107–14.
[14] Motalleb M, Ghorbani R. Non-cooperative game-theoretic model of demand response aggregator competition for selling stored energy in storage devices. Appl Energy 2017;202:581–96.
[15] Tan Z, Ju L, Li H, Zhang H. A two-stage scheduling optimization model and solution algorithm for wind power and energy storage system considering uncertainty and demand response. Int J Electr Power Energy Syst 2016;63:1057–69.
[16] Hatami A, Seifi H, Sheikh-El-Eslami ML. A stochastic-based decision-making framework for an electricity retailer: time-of-use pricing and electricity portfolio optimization. IEEE Trans Power Syst 2011;26(4):1808–16.

[17] Peng Y, Tang G, Nehorai A. A game-theoretic approach for optimal time-of-use electricity pricing. IEEE Trans Power Syst 2013;28(2):884–92.
[18] Bae KY, Han HS, Dan DK. Hourly solar irradiance prediction based on support vector machine and its error analysis. IEEE Trans Power Syst 2017;32(2):935–45.
[19] Adika CO, Wang L. Autonomous appliance scheduling based on time of use probabilities and load clustering. 10th Int'l power and energy conf. 2012. p. 42–7.
[20] Atia R, Yamada N. Sizing and analysis of renewable energy and battery systems in residential microgrids. IEEE Trans Smart Grid 2016;7(3):1204–13.
[21] Choi JW, Heo SY, Kim MK. Hybrid operation strategy of wind energy storage system for power grid frequency regulation. IET Gener Transm Distrib 2016;10(3):736–49.
[22] Zhang F, Wang G, Meng K, Zhao J, Xu Z, Dong Z, et al. Improved cycle control and sizing scheme for wind energy storage system based on multi-objective optimization. IEEE Trans Sustain Energy 2016;8(3):966–77.
[23] Korkas CD, Baldi S, Michailidis I, Kosmatopoulos EB. Occupancy-based demand response and thermal comfort optimization in microgrids with renewable energy sources and energy storage. Appl Energy 2016;163:93–104.
[24] Manchester S, Barzegar B, Swan L, Groulx D. Energy storage requirements for in-stream tidal generation on a limited capacity electricity grid. Energy 2013;61:283–90.
[25] Chen Y, Zheng Y, Luo F, et al. Reliability evaluation of distribution systems with mobile energy storage systems. IET Renew Power Gener 2017;10(10):1562–9.
[26] Bahramirad S, Reder W, Khodaei A. Reliability-constrained optimal sizing of energy storage system in a microgrid. IEEE Trans Smart Grid 2012;3(4):2056–62.
[27] Arabali A, Ghofrani M, Etezadi-Amoli M, Fadali M. Stochastic performance assessment and sizing for a hybrid power system of solar/wind/energy storage. IEEE Tran Sustain Energy 2014;5(2):363–71.
[28] Paliwal P, Patidar NP, Nema RK. A novel method for reliability assessment of autonomous PV-wind-storage system using probabilistic storage model. Int J Electr Power Energy Syst 2014;55(2):692–703.
[29] Hu P, Karki R, Billinton R. Reliability evaluation of generating systems containing wind power and energy storage. IET Gener Transm Distrib 2009;3(8):783–91.
[30] Milad ZG, Farshad K, Mehdi A, Behnam MI. Reliability assessment of generating systems containing wind power and air separation unit with cryogenic energy storage. J Energy Storage 2018;16:116–24.
[31] Arasteh F, Riahy GH. MPC-based approach for online demand side and storage system management in market based wind integrated power systems. Int J Electr Power Energy Syst 2019;106:124–37.
[32] Yang Hejun, Wang Lei, Zhang Yeyu, et al. Reliability evaluation of power system considering time of use electricity pricing. IEEE Trans Power Syst 2018. [Early Access].
[33] Lazinica A. Particle swarm optimization. Vienna (VIE, Austria): In-Tech; 2009.
[34] Cheng S, Chen MY. Multi-objective reactive power optimization strategy for distribution system with penetration of distributed generation. Int J Electr Power Energy Syst 2014;62:221–8.
[35] Clerc M. Particle swarm optimization. London (LON, UK): ISTE Ltd; 2006 Bhuiyan FA, Yazdani A. Reliability assessment of a wind-power system with integrated energy storage. IET Renew Power Gener 2010;4(3):211–20.
[36] Billinton R, Allan R. Reliability evaluation of power system. New York (NY, USA): Plenum; 1996.